A muscovite-biotite geothermometer

Thomas D. Hoisch

Department of Geology, Northern Arizona University, Flagstaff, Arizona 86011-6030, U.S.A.

Abstract

A geothermometer based on the exchange of Mg-Tschermak's component between muscovite and biotite ($[MgSiAl_{-2}]^B = [MgSiAl_{-2}]^M$) is empirically calibrated using data from 43 rocks having the assemblage muscovite + biotite + quartz + plagioclase + garnet + Al_2SiO_5. Temperatures and pressures for the calibration are determined through the simultaneous application of garnet-biotite geothermometry and GASP geobarometry.

Multiple regression is used to solve for unknowns in the equilibrium thermodynamic expression. Incorporated into the expression are interaction parameters that model nonideality in the mixing of cations within the octahedral sites of both muscovite and biotite. With temperature chosen as the dependent variable, this yields

$$T = \frac{500.110 + 0.0147890P - 878.745(X^B_{Mg} - X^B_{[6]Al}) - 4532.67[X^M_{Mg}(X^M_{Mg} - 2)]}{1 + 0.0237527R \ln K},$$

where P is in bars, T in kelvins, $R = 8.3144$ J/K, X^m_Q denotes mole fraction Q in the octahedral site for mineral m (M = muscovite, B = biotite), and

$$K = 27[(Mg/^{[6]}Al)^M/(Mg/^{[6]}Al)^B].$$

The quality of fit is indicated by a multiple correlation coefficient of 0.92. A standard deviation of 22 K in the residuals may be easily explained through the propagation of errors associated with microprobe analysis. Use of the muscovite-biotite geothermometer should be restricted to micas that are compositionally similar to those in the calibration data set.

Introduction

Many studies have investigated the petrologic significance of compositional variations within muscovite and biotite (Speer, 1984; Guidotti, 1984). In metapelites, muscovite has been found to vary in composition as a function of metamorphic grade, these variations sometimes involving maxima or minima (Guidotti and Sassi, 1976; Guidotti, 1978). One prominent trend in both muscovite and biotite is the tendency for Ti content to increase with grade in the presence of a Ti-saturating phase (Guidotti et al., 1977; Guidotti, 1978). High-Ti muscovites are also characteristic of two-mica granites (Miller et al., 1981; Anderson and Rowley, 1981), suggesting that the Ti-enrichment trend continues to higher temperatures and to coexistence with melts. Theoretical studies (e.g., Thompson, 1976) have predicted the nature of biotite Fe-Mg variations in the prograde metamorphism of pelitic rocks, and such variations have been observed (e.g., Triboulet and Audren, 1985). One previous study has addressed the partitioning of Ti between coexisting muscovite and biotite and found little temperature sensitivity (Guidotti et al., 1977). Pattison (1987) found that net-transfer reactions involving the Tschermak's components of muscovite, biotite, and chlorite explain systematic

compositional variations in pelitic rocks in the Ballachullish thermal aureole, Scotland. Systematic compositional variations within muscovite and biotite as a function of metamorphic grade imply that equilibria involving components of the two minerals may be sensitive monitors of physical conditions.

The present study uses a thermodynamic approach and empirical calibration to investigate the reaction involving the exchange of Mg-Tschermak's component between coexisting muscovite and biotite ($[MgSiAl_{-2}]^B = [MgSiAl_{-2}]^M$) as a possible geothermometer. In terms of end-member components, this reaction may be written as

$$KMg_3(AlSi_3)O_{10}(OH)_2 + KAl_2(AlSi_3)O_{10}(OH)_2$$

Phlogopite   Muscovite

$$= K(MgAl)Si_4O_{10}(OH)_2 + K(Mg_2Al)(Al_2Si_2)O_{10}(OH)_2,$$

Celadonite   Eastonite

(R1)
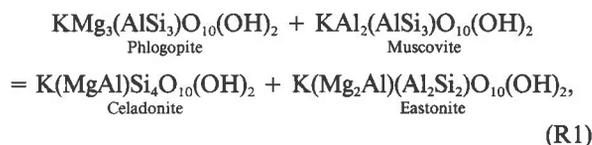
where the equilibrium constant is given by

$$K_{R1} = a_{cel}a_{eas}/ a_{phl}a_{ms}.$$

The treatment of nonideality in the activity-composition relations of micas is facilitated by subdividing K_{R1} into

TABLE 1. Microprobe analyses of minerals

	Muscovite*		Biotite*			Garnet**			Plagioclase*	
	CC-33a	CC-36	CC-33a	CC-36		CC-33a	CC-36		CC-33a	CC-36
SiO_2	44.690	45.030	34.680	34.866	SiO_2	37.066	37.544	SiO_2	63.141	64.850
Al_2O_3	32.705	32.260	17.456	17.158	Al_2O_3	20.730	20.425	Al_2O_3	23.465	22.110
TiO_2	0.785	0.695	2.428	2.014	TiO_2	0.004	0.000	FeO	0.023	0.016
MgO	0.788	0.705	9.947	10.596	MgO	3.562	3.845	Na_2O	9.445	10.411
FeO	1.495	2.315	19.600	20.298	FeO	33.643	32.523	K_2O	0.056	0.046
MnO	0.020	0.000	0.019	0.620	Fe_2O_3	0.478	0.903	CaO	4.870	3.267
Na_2O	1.350	1.800	0.302	0.308	MnO	1.916	3.550			
K_2O	9.730	9.205	9.369	9.042	CaO	1.832	1.355			
CaO	0.003	0.010	0.001	0.000						
F	0.108	0.035	0.615	0.558						
Total	91.627†	92.040†	94.159†	94.667†		99.231	100.145		101.000	100.700
Si	3.105	3.120	2.698	2.701	Si	2.998	3.011	Si	2.772	2.844
Al	2.678	2.635	1.601	1.567	Al	1.976	1.930	Al	1.214	1.143
Ti	0.041	0.036	0.142	0.117	Ti	0.000	0.000	Fe^{2+}	0.001	0.001
Mg	0.082	0.073	1.154	1.223	Mg	0.429	0.459	Na	0.804	0.885
Fe^{2+}	0.087	0.134	1.276	1.316	Fe^{2+}	2.276	2.182	K	0.003	0.003
Mn	0.001	0.000	0.001	0.004	Fe^{3+}	0.029	0.054	Ca	0.229	0.154
Na	0.182	0.242	0.046	0.046	Mn	0.131	0.241			
K	0.862	0.814	0.930	0.893	Ca	0.159	0.116			
Ca	0.000	0.001	0.000	0.000						
F	0.024	0.008	0.151	0.137						
Oxygen‡	11	11	11	11		12	12		8	8

Note: Sample locations, CC-33a: Funeral Mountains, California, lat 36°43'6"N, long 116°55'35"W; CC-36: Funeral Mountains, California, lat 36°43'13"N, long 116°55'26"W.
* All Fe as Fe^{2+}.
** Fe^{2+} and Fe^{3+} calculated by charge balance assuming 12 oxygens and 8 cations.
† Total minus weight of oxygen charge-equivalent of fluorine.
‡ Normalization to number of anhydrous oxygens indicated.

two terms, a term comprising ideal activity models, K_{R1}^{ideal}, and a term comprising activity coefficients, $K_{R1,\gamma}$:

$$K_{R1} = K_{R1}^{ideal} K_{R1,\gamma}$$

where

$$K_{R1}^{ideal} = X_{cel} X_{eas} / X_{phl} X_{ms}$$

and

$$K_{R1,\gamma} = \gamma_{cel} \gamma_{eas} / \gamma_{phl} \gamma_{ms}. \qquad (1)$$

DATA SET

The present study makes use of previously published mineral composition data on 41 rocks having the mineral assemblage muscovite + biotite + quartz + garnet + plagioclase + Al_2SiO_5. Data from two rocks from the Funeral Mountains, California (this study), are included in the data set (Table 1). Data from the published literature were selected for this study based on the completeness of the mica analyses (at least oxides of Al, Si, Mg, Fe^{2+}, Ti, K, and Na) (Table 2). As done in the study of Hodges and Crowley (1985), rim compositions of garnets were used whenever analyses were given for both rims and cores. Maximum ranges of composition were reported for garnet and plagioclase from the study of Fletcher and Greenwood (1979). For each sample in that study, the most calcic plagioclase composition was chosen as the equilibrium composition, in accordance with their observation of reverse zoning and generally increasing anorthite content with metamorphic grade. Also, garnet compositions showing higher Fe and Mg combined with lower

Mn (or two out of three when ambiguous) were taken as equilibrium compositions, these being likely to reflect rims as judged by several line traverses given in Fletcher and Greenwood's study. For use in the present study, Fe^{2+} and Fe^{3+} content were calculated for all garnets by charge balance (see Table 1). For micas, all Fe was assumed to be Fe^{2+}, and normalization was to 11 anhydrous oxygens.

EMPIRICAL CALIBRATION

Estimation of pressures and temperatures

From the data set, pressures and temperatures were determined on each sample through the simultaneous application of the garnet-biotite geothermometer (R2) and the GASP geobarometer (R3):

$$\underset{\text{Almandine}}{Fe_3Al_2Si_3O_{12}} + \underset{\text{Phlogopite}}{KMg_3(AlSi_3)O_{10}(OH)_2} \qquad (R2)$$
$$= \underset{\text{Pyrope}}{Mg_3Al_2Si_3O_{12}} + \underset{\text{Annite}}{KFe_3(AlSi_3)O_{10}(OH)_2}$$

$$\underset{\text{Anorthite}}{3\,CaAl_2Si_2O_8} = \underset{\text{Quartz}}{SiO_2} + \underset{\substack{\text{Kyanite or}\\\text{Sillimanite}}}{2\,Al_2SiO_5} + \underset{\text{Grossular}}{Ca_3Al_2Si_3O_{12}}.$$
$$(R3)$$
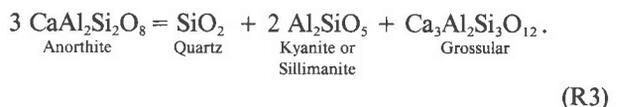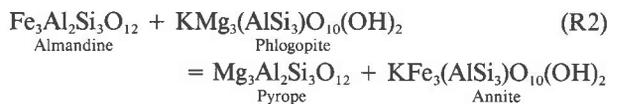
To calculate the equilibrium temperature and pressure for each of the 43 samples, the equilibrium thermodynamic expressions for R2 and R3 were solved simultaneously. Each takes the form

$$0 = \Delta H - T\Delta S + P\Delta V + RT \ln K. \qquad (2)$$

TABLE 2. Calibration data set

Reference	Sample	Phase in R3*	Actual phases**	T (°C)	P (bars)	K_{R1}^{ideal}	X_{Mg}^B	X_{BIAl}^B	X_{Ti}^B	X_{Fe}^B	X_{Mg}^M
Hodges and	79-78B	Sil	Sil	472	3921	0.298	0.377	0.168	0.0271	0.387	0.0235
Spear (1982)	79-80D	Sil	Sil	499	3277	0.278	0.372	0.151	0.0240	0.430	0.0240
	79-90A	Sil	Sil	491	3858	0.277	0.393	0.162	0.0246	0.387	0.0237
	79-92D	Sil	Sil	497	4257	0.294	0.373	0.162	0.0263	0.407	0.0238
	79-145E	Sil	Sil	504	4095	0.305	0.330	0.161	0.0272	0.443	0.0221
	79-146B	Sil	And-Sil	537	3437	0.218	0.416	0.162	0.0263	0.360	0.0199
	79–146D	Sil	And-Sil	468	2059	0.287	0.417	0.161	0.0245	0.361	0.0260
Tracy (1978)	892U	Sil	Sil	588	4086	0.380	0.363	0.130	0.0560	0.398	0.0365
	869	Sil	Sil	538	3262	0.344	0.362	0.129	0.0613	0.388	0.0329
	871	Sil	Sil	596	3583	0.394	0.332	0.128	0.0660	0.408	0.0350
	C26A	Sil	Sil	566	2678	0.313	0.347	0.111	0.0558	0.439	0.0337
	595C	Sil	Sil	752	6933	0.380	0.400	0.119	0.0656	0.351	0.0433
	M34	Sil	Sil	520	4003	0.249	0.367	0.099	0.0732	0.400	0.0311
Pigage (1982)	373	Ky	Ky	554	5473	0.361	0.368	0.141	0.0364	0.414	0.0330
	121	Ky	Ky	547	4840	0.386	0.376	0.145	0.0383	0.397	0.0346
	367	Ky	Ky-Sil	564	6061	0.393	0.382	0.147	0.0365	0.387	0.0352
	82	Ky	Ky-Sil	531	4491	0.417	0.363	0.151	0.0407	0.394	0.0346
	398	Sil	Sil	547	4390	0.374	0.357	0.147	0.0368	0.410	0.0316
	492	Ky	Ky-Sil	543	4382	0.288	0.372	0.149	0.0381	0.394	0.0252
	223	Ky	Ky-Sil	536	4278	0.377	0.384	0.148	0.0333	0.394	0.0338
	2-376	Ky	Ky-Sil	565	5748	0.361	0.370	0.142	0.0426	0.398	0.0325
	2-13	Sil	Sil	530	4632	0.382	0.351	0.143	0.0411	0.414	0.0322
	74	Sil	Sil	589	5684	0.360	0.373	0.125	0.0485	0.407	0.0363
	59	Sil	Sil	564	5504	0.395	0.364	0.146	0.0439	0.393	0.0339
	40	Sil	Sil	552	4595	0.335	0.374	0.147	0.0393	0.400	0.0295
Pigage (1976)	2	Ky	Ky	536	6310	0.124	0.388	0.170	0.0329	0.342	0.0100
	3	Ky	Ky	604	7684	0.108	0.375	0.170	0.0331	0.352	0.0085
	4	Ky	Ky	559	7655	0.153	0.395	0.168	0.0329	0.339	0.0125
	5	Ky	Ky	575	5498	0.126	0.365	0.164	0.0372	0.362	0.0099
	6	Ky	Ky	565	5211	0.145	0.366	0.168	0.0388	0.350	0.0110
	7	Sil	Sil	600	5386	0.122	0.362	0.165	0.0402	0.356	0.0094
Fletcher and	5	Ky	Ky	657	7674	0.499	0.373	0.148	0.0380	0.387	0.0431
Greenwood	6	Ky	Ky	541	5429	0.445	0.389	0.167	0.0306	0.346	0.0360
(1979)	7	Ky	Ky	683	5152	0.413	0.400	0.152	0.0324	0.369	0.0375
	8	Ky	Ky	618	7546	0.406	0.403	0.146	0.0330	0.369	0.0382
	9	Ky	Ky	530	4136	0.435	0.397	0.161	0.0341	0.350	0.0371
	11	Ky	Ky	576	7039	0.390	0.400	0.142	0.0375	0.367	0.0376
	12	Ky	Ky	608	5852	0.413	0.383	0.160	0.0356	0.367	0.0343
	13	Ky	Ky	728	9585	0.341	0.402	0.143	0.0383	0.376	0.0336
	14	Ky	Ky	665	8409	0.438	0.342	0.146	0.0442	0.412	0.0353
	15	Sil	Sil	649	7677	0.475	0.319	0.154	0.0411	0.427	0.0336
This study	CC-33a	Ky	Ky	655	7429	0.320	0.385	0.100	0.0474	0.425	0.0408
	CC-36	Ky	Ky	693	8966	0.246	0.408	0.089	0.0390	0.439	0.0364

* Eq. 4 was used where kyanite is listed; Eq. 5 was used where sillimanite is listed.
** Al$_2$SiO$_5$ phases present: And = andalusite, Ky = kyanite, Sil = sillimanite.

Equation 2 assumes that the heat capacity of reaction (ΔC_P) is zero and that the volume of reaction does not vary as a function of pressure and temperature. Using joule and bar quantities, the equilibrium thermodynamic expression for R2 given by Ferry and Spear (1978) is

$$0 = 52\,108 - 19.506T + 0.2385P + RT \ln K_{R2}, \quad (3)$$

where $K_{R2} = a_{py}X_{ann}/a_{al}X_{phl}$.

Equilibrium thermodynamic expressions for R3 may be derived through the algebraic manipulation of equations given in the study of Koziol and Newton (1988). For kyanite, the expression is

$$0 = -45\,462.29 + 141.588T + (V_{gr} - 18.74)P + RT \ln K_{R3}, \quad (4)$$

and for sillimanite, the expression is

$$0 = -33\,157.78 + (121.182 - 0.000\,965T)T + (V_{gr} - 17.684)P + RT \ln K_{R3}, \quad (5)$$

where $K_{R3} = a_{gr}/(a_{an})^3$ and V_{gr} is the partial molar volume (J/bar) of the grossular component calculated using the method of Newton and Haselton (1981), as adjusted by Hodges and Crowley (1985).

Because the activity-composition models for garnet and plagioclase selected for this study are temperature dependent, the simultaneous solution of Equations 3 and 4 or 3 and 5 required iteration, with the first iteration assuming a temperature of 500 °C, and the subsequent iterations using the temperature calculated from the previous iteration until convergence (less than 0.01-K difference) was achieved. Using the activity models discussed below and the Al$_2$SiO$_5$ stability fields of Holdaway (1971), the

pressures and temperatures calculated place all samples except two within 20 °C or 300 bars of the proper field or within one of the two fields if two Al_2SiO_5 phases are present in the rock (Fig. 1).

Activity-composition relations

Ideal mixing-on-sites models (e.g., Powell, 1978; Price, 1985) that consider mixing in the octahedral sites were used to calculate ideal activities for the phase components of muscovite and biotite. The interlayer sites may be disregarded because their terms cancel out in the expressions of K_{R1}^{ideal} and K_{R2}. Similarly, terms involving the tetrahedral sites cancel out in the expression of K_{R2}. Excluding the tetrahedral sites in the activities used to calculate K_{R1}^{ideal} yielded a significantly better fit in the regression over when they were included. Hence, the tetrahedral sites were excluded from the activity expressions in micas for all applications in the present study.

For the activity of anorthite in plagioclase, the model of Newton et al. (1980) was used. For garnet, the models of Hodges and Spear (1982), Ganguly and Saxena (1984), and Grambling (1986) were tested in combination with the above to see which provided the best correspondence between the calculated pressure and temperature and the stability field of the Al_2SiO_5 phase in the rock. Using the Al_2SiO_5 stability fields given by Holdaway (1971), the models of Hodges and Spear (1982) produced the best correspondence (Fig. 1). Table 3 summarizes the activity models used in this study.

Regression

Unknowns in the thermodynamic expression of R1 were solved using multiple regression. To perform the regression, a system of equations based on Equation 2 is needed, one equation for each sample. Before the regression can be performed, the equilibrium thermodynamic expression (Eq. 2) must be elaborated to involve nonideality in the mixing of cations within the octahedral sites of both muscovite and biotite.

To evaluate $RT \ln[\gamma_{eas}/\gamma_{phl}]$ (part of the expression of $RT \ln K_{R1,\gamma}$), a method based on the work of Ganguly and Kennedy (1974) was used. Using the symmetric "simple mixture" model of Guggenheim (1967), Ganguly and Kennedy (1974) derived an expression appropriate for the mixing of four species on one site. In biotite, this expression may be applied to the octahedrally coordinated constituents Al, Mg, Fe^{2+}, and Ti:

$$RT \ln[\gamma_{eas}/\gamma_{phl}] = W_{Mg-Al}^B(X_{Mg}^B - X_{[6]Al}^B) + \Delta W_{Ti}^B X_{Ti}^B + \Delta W_{Fe}^B X_{Fe}^B, \qquad (6)$$

where $\Delta W_{Ti}^B = W_{Al-Ti}^B - W_{Mg-Ti}^B$ and $\Delta W_{Fe}^B = W_{Al-Fe}^B - W_{Mg-Fe}^B$ and the compositional variable X indicates mole fraction in the octahedral sites based on three octahedral sites.

To evaluate activity coefficients for the MgAl-celadonite component in muscovite, a different treatment was preferred because of the very low concentrations of Mg. The mole fraction of Mg in the octahedral sites in mus-

covite is typically about 0.03 (Table 2), implying Henry's law behavior of the MgAl-celadonite component. A treatment applicable to phase components whose theoretical end-members involve trace elements (Powell, 1978, p. 51) was used to formulate an expression for $RT \ln \gamma_{cel}$:

$$RT \ln \gamma_{cel} = W_{Mg}^M[X_{Mg}^M(X_{Mg}^M - 2)], \qquad (7)$$

where the compositional variable X_{Mg}^M denotes the mole fraction of Mg in the octahedral sites based on two octahedral sites. Because the value of W_{Mg}^M would vary with major variations in the overall muscovite composition, this approach is valid only if all muscovite compositions used are similar. All muscovites used in the present study are composed primarily of end-member muscovite component, with only minor compositional variations occurring within the data set.

Taking the activity coefficient of the muscovite component to be 1, the full equilibrium thermodynamic expression for R1 may now be written from Equations 1, 2, 6, and 7:

$$0 = \Delta H - T\Delta S + P\Delta V + RT \ln K_{R1}^{ideal}$$
$$+ W_{Mg-Al}^B(X_{Mg}^B - X_{[6]Al}^B) + \Delta W_{Ti}^B X_{Ti}^B$$
$$+ \Delta W_{Fe}^B X_{Fe}^B + W_{Mg}^M[X_{Mg}^M(X_{Mg}^M - 2)]. \qquad (8)$$

K_{R1}^{ideal} may be simplified from the activity models in Table 3:

$$K_{R1}^{ideal} = 27[(Mg/^{[6]}Al)^M/(Mg/^{[6]}Al)^B].$$

To perform the regression, Equation 8 is rewritten to make temperature the dependent variable:

$$T = \Delta H/\Delta S + P\Delta V/\Delta S + RT \ln K_{R1}^{ideal}/\Delta S$$
$$+ (W_{Mg-Al}^B/\Delta S)(X_{Mg}^B - X_{[6]Al}^B)$$
$$+ (\Delta W_{Ti}^B/\Delta S)X_{Ti}^B + (\Delta W_{Fe}^B/\Delta S)X_{Fe}^B$$
$$+ (W_{Mg}^M/\Delta S)[X_{Mg}^M(X_{Mg}^M - 2)]. \qquad (9)$$

From this, one equation for each of the 43 samples is formulated using P, T, K_{R1}^{ideal}, and compositional data (Table 2). In this form, multiple regression finds solutions to $\Delta H/\Delta S$, $\Delta V/\Delta S$, $1/\Delta S$, $W_{Mg-Al}^B/\Delta S$, $\Delta W_{Ti}^B/\Delta S$, $\Delta W_{Fe}^B/\Delta S$, and $W_{Mg}^M/\Delta S$ that minimize the sum of squares of residuals of temperature, resulting in the best possible geothermometer.

An iterative approach was needed to regress unknowns in Equation 9 because the variable T could not be factored out in such a way as to produce coefficients of discrete numbers. Without iteration, temperatures calculated using the regressed variables would not be the same as those used to calculate the values of $RT \ln K_{R1}^{ideal}$, as they must if regressed variables are to be used to solve uniquely for temperature. To treat this problem, temperatures calculated from the regressed variables were used to recalculate $RT \ln K_{R1}^{ideal}$ values, which were then used to regress variables again. This continued until the differences between temperatures calculated from regressed
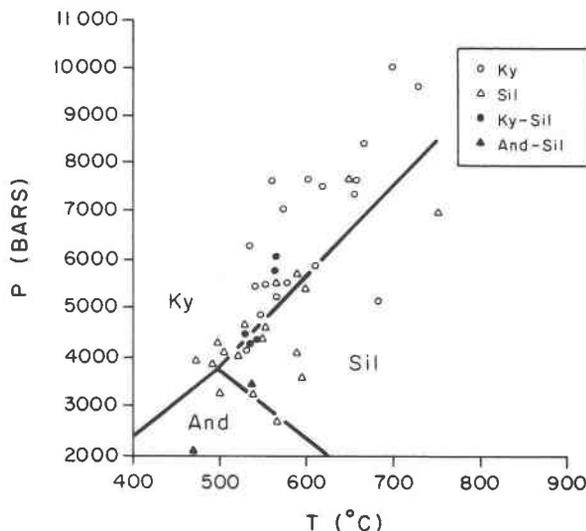
Fig. 1. Pressures and temperatures calculated for data set showing aluminum silicate phases (Ky = kyanite, Sil = sillimanite, And = andalusite) relative to stability fields of Holdaway (1971).

TABLE 3. Activity models

Micas

$$X_{cel} = 4X_{Mg}^M X_{[6]Al}^M$$
$$X_{ms} = (X_{[6]Al}^M)^2$$
$$X_{eas} = 6.75(X_{Mg}^B)^2 X_{[6]Al}^B$$
$$X_{phl} = (X_{Mg}^B)^3$$
$$X_{ann} = (X_{Fe}^B)^3$$

where $X_{Mg}^M = Mg/2$; $X_{[6]Al}^M = (Al + Si - 4)/2$
$X_{Mg}^B = Mg/3$; $X_{[6]Al}^B = (Al + Si - 4)/3$
$X_{Fe}^B = Fe/3$

Garnet

$$a_{py} = \langle X_{py}\exp\{[(3300 - 1.5T)/RT] (X_{gr}^2 + X_{al}X_{gr} + X_{gr}X_{sp})\}\rangle^3$$
$$a_{al} = \langle X_{al}\exp\{[(1.5T - 3300)/RT] X_{py}X_{gr})\rangle^3$$
$$a_{gr} = \langle X_{gr}\exp\{[(3300 - 1.5T)RT] (X_{py}^2 + X_{al}X_{py} + X_{py}X_{sp})\}\rangle^3$$

where T is in kelvins, R = 1.987 cal/K, and

$$X_{py} = Mg/(Mg + Fe^{2+} + Ca + Mn)$$
$$X_{al} = Fe^{2+}/(Mg + Fe^{2+} + Ca + Mn)$$
$$X_{gr} = Ca/(Mg + Fe^{2+} + Ca + Mn)$$
$$X_{sp} = Mn/(Mg + Fe^{2+} + Ca + Mn)$$

Plagioclase

$$a_{an} = [X_{an}(1 + X_{an})^2/4] \exp\{[(1 - X_{an})^2/RT] (2050 + 9392X_{an})\}$$

where T is in kelvins, R = 1.987 cal/K, $X_{an} = Ca/(Ca + Na + K)$

variables in successive iterations were less than 0.1 °C for all samples. Throughout the procedure, the values assigned to the dependent variable T remained those determined using garnet-biotite geothermometry (Table 2). This procedure insured that temperatures calculated from the regressed variables were within 0.1 °C of those used to calculate the values of $RT \ln K_{R1}^{ideal}$.

Uncertainties associated with the determinations of $\Delta W_{Ti}^B/\Delta S$ and $\Delta W_{Fe}^B/\Delta S$ indicated no significance for these variables. These were eliminated using a stepwise procedure with backward elimination (e.g., Devore, 1982, p. 500). By examining residual plots, four samples were found to be discrepant: 79-146B, 595C, and samples 7 and 13 of Fletcher and Greenwood (1979). Elimination of these from the data set caused a dramatic improvement in the quality of fit. The results of the final regression are $\Delta H/\Delta S$ = 500.110 ± 43.529 K, $\Delta V/\Delta S$ = 0.0147890 ± 0.0028380 K/bar, $1/\Delta S$ = −0.0237527 ± 0.0042106 K/J, $W_{Mg-Al}^B/\Delta S$ = −878.745 ± 202.304 K, and $W_{Mg}^M/\Delta S$ = −4532.67 ± 703.46 K with 1σ uncertainties indicated. A multiple correlation coefficient of 0.92 is derived from the regression, as is a standard deviation of 22 K in the residuals.

A geothermometric expression in which temperature is solved given pressure and compositional data may be formulated from the regressed variables by rearranging Equation 9:

In order for Equation 10 to be useful as a geothermometer, temperatures calculated must be insensitive to uncertainties in the assumed pressure. The sensitivity of the calculated temperature to pressure may be evaluated by differentiating Equation 10:

$$dT/dP = 0.0147890(1 + 0.0237527R \ln K_{R1}^{ideal}). \quad (11)$$

For the end-member reaction ($\ln K_{R1}^{ideal} = 0$), dT/dP = 0.0147890 K/bar, indicating that a 1-kbar uncertainty in pressure propagates to a 14.8-K uncertainty in temperature. This compares to a 12.2-K uncertainty for the end-member garnet-biotite exchange reaction ($\ln K_{R2} = 0$, dT/dP = 0.01223 K/bar). Thus, the muscovite-biotite geothermometer has little sensitivity to pressure, but slightly more than the garnet-biotite geothermometer.

Temperatures calculated using the regressed variables are compared to temperatures used in the calibration in Figure 2. For all 39 samples, the difference is less than 38 K. For 20 samples, it is less than 20 K. The high multiple correlation coefficient of 0.92 is reflected in the small scatter of data about a line of hypothetical perfect correlation (Fig. 2).

Discussion of uncertainties

There are numerous possible sources of error that might contribute to the scatter of data about the best-fit "surface." These include uncertainties in the mineral analyses, uncertainties in the activity-composition models for

$$T = \frac{500.110 + 0.0147890P - 878.745(X_{Mg}^B - X_{[6]Al}^B) - 4532.67[X_{Mg}^M(X_{Mg}^M - 2)]}{1 + 0.0237527R \ln K_{R1}^{ideal}}. \quad (10)$$
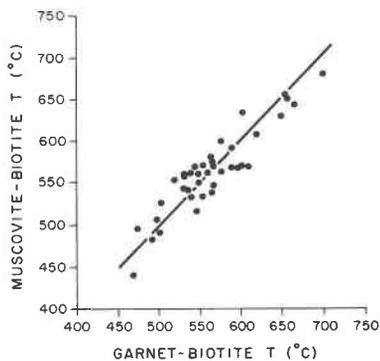
Fig. 2. Residual plot comparing temperatures calculated using the muscovite-biotite geothermometer (R1) and garnet-biotite geothermometer (R2) for the 39 samples used in the calibration of R1. Line represents hypothetical perfect correlation.

the solid-solution phases, uncertainties introduced by possible disequilibrium among the phases, uncertainties introduced by assuming $\Delta C_P = 0$, and uncertainties introduced by assuming that ΔV does not vary with pressure and temperature. Uncertainties introduced by the latter two are probably very small. Uncertainties in the experimental calibrations of R2 and R3 are systematic in nature and hence do not contribute to the scatter of data about the best-fit "surface," but make very important contributions to the total uncertainty for any calculated values of pressure or temperature (Hodges and McKenna, 1987).

The only source of nonsystematic errors that may be independently quantified is that introduced by the electron-microprobe analysis of minerals. Whether this source of errors explains the scatter of data about the best-fit "surface" may be easily tested. By propagating analytical errors through the muscovite-biotite geothermometer (R1) and the garnet-biotite geothermometer (R2), the error associated with the difference between the two may be predicted and compared to the standard deviation of the residuals of 22 K derived from the regression of thermodynamic variables. A minimal estimate of analytical errors is obtainable from counting statistics. Unfortunately, counting statistics were not reported for most of the data used in the calibration, so the assumption will be made that counting statistics are similar to those for the data in Table 2. Counting statistics for the microprobe analyses in Table 2 are 1% for those elements that could achieve this in less than 40-s counting time. This precision could not be achieved for some elements that occur in low concentrations. Counting statistics for Mg in muscovite are 3%, and in garnet, counting statistics for Mg are 1.1%, Ca 1.6%, and Mn 3%. One study (M. Kohn, 1988, personal communication) has shown that the total error in microprobe analysis is typically two to three times the counting statistics when comparing different data sets taken on the same machine. In the present study, analyt-

ical errors should be even larger because the calibration data set comprises data taken on different machines. Using the minimal assumption that analytical errors are twice the counting statistics, the Monte Carlo method of error propagation (Anderson, 1976, 1977) determines a 1σ uncertainty of 13 K for applications of the garnet-biotite geothermometer (σ_{R2}), and a 1σ uncertainty of 20 K for the muscovite-biotite geothermometer (σ_{R1}). From these, the error associated with the difference between temperatures calculated using R1 and R2 (σ_{R1-R2}) may be determined using the following approximate relation:

$$(\sigma_{R1-R2})^2 = (\sigma_{R1})^2 + (\sigma_{R2})^2 + 2\rho\sigma_{R1}\sigma_{R2}, \qquad (12)$$

where ρ is the coefficient of correlation between the R1 and R2 errors (Anderson, 1977). A value of 24 K for σ_{R1-R2} is calculated when no correlation of errors is assumed ($\rho = 0$). A comparison with the error of 22 K in the residuals (discussed above) indicates that errors stemming from the microprobe analysis of minerals easily explain all of the scatter of data about the best-fit "surface."

RESTRICTIONS ON THE USE OF MUSCOVITE-BIOTITE GEOTHERMOMETER

Although experience with applications of the muscovite-biotite geothermometer will ultimately determine the circumstances under which it can be reliably applied, some restrictions may be inferred. One important restriction concerns the applicable ranges of mica compositions. In the calibration data set, micas are Al rich and show only narrow ranges of composition. This is a consequence of Al saturation by coexisting Al_2SiO_5 phases and of occurrence within very similar low-variance mineral assemblages. The interaction parameter W_{Mg}^M is valid only for muscovite that is similar compositionally to muscovites in the calibration data set. The assumption of a symmetric mixing model for octahedrally coordinated species in biotite appears to have validity over the narrow range of compositions in the calibration data set, but extrapolation beyond this must be questioned. In view of these considerations, applications should be restricted to micas whose compositions fall within the ranges of the calibration data set (see Table 4).

The 39 samples used in the final regression cover physical conditions ranging from 450 to 700 °C and 2000 to 9600 bars. The use of Equation 10 at conditions outside these, or at conditions unrepresented in the data set such as blueschist-facies metamorphism, involves higher uncertainties than other applications. The uncertainty associated with any application, taking this effect into consideration, may be evaluated by calculating the prediction interval **P** (e.g., Devore, 1982, p. 445–446, 511–512):

$$\mathbf{P} = t_{\alpha/2}[\sigma^2(1 + \mathbf{x}'(\mathbf{X}'\mathbf{X})^{-1}\mathbf{x})]^{1/2}, \qquad (13)$$

where $t_{\alpha/2}$ is the Student's t-value for 34 degrees of freedom, α is 1 minus the desired confidence level, $\sigma = 22.3$ K (standard deviation of the residuals), and

$$\mathbf{x}' = [1 \quad P \quad RT \ln K_{R1}^{ideal} \quad X_{Mg}^{B} - X_{[6]Al}^{B} \quad X_{Mg}^{M}(X_{Mg}^{M} - 2)]$$

$$\mathbf{x} = \begin{bmatrix} 1 \\ P \\ RT \ln K_{R1}^{ideal} \\ X_{Mg}^{B} - X_{[6]Al}^{B} \\ X_{Mg}^{M}(X_{Mg}^{M} - 2) \end{bmatrix}$$

$$(\mathbf{X'X})^{-1} = \begin{bmatrix} 3.81 & 8.08 \times 10^{-5} & 2.66 \times 10^{-4} & 1.75 & 41.9 \\ 8.08 \times 10^{-5} & 1.62 \times 10^{-8} & 1.51 \times 10^{-8} & 4.30 \times 10^{-4} & 2.41 \times 10^{-3} \\ 2.66 \times 10^{-4} & 1.51 \times 10^{-8} & 3.57 \times 10^{-8} & 1.22 \times 10^{-3} & 5.68 \times 10^{-3} \\ 1.75 & 4.30 \times 10^{-4} & 1.22 \times 10^{-3} & 82.4 & 219 \\ 41.9 & 2.41 \times 10^{-3} & 5.68 \times 10^{-3} & 219 & 996 \end{bmatrix}.$$

$\mathbf{x}'$ is the vector of coefficients used to set up the coefficient matrix in the final regression, $\mathbf{x}$ is the transpose of $\mathbf{x}'$, and $(\mathbf{X'X})^{-1}$ is the coefficient matrix used in the final regression multiplied by its transpose and inverted. For example, applying Equations 10 and 13 to sample 79-78B, assuming a 90% confidence level ($t_{\alpha/2} = 1.693$) and using the data in Table 2, the calculated muscovite-biotite temperature and 90% prediction interval are 495 ± 39.6 °C.

CONCLUSIONS

The exchange of Mg-Tschermak's component between muscovite and biotite is found through empirical calibration to have a strong temperature dependence, weak pressure dependence, and utility as a geothermometer. Unknowns in the equilibrium thermodynamic expression were determined by using multiple regression, incorporating terms that model nonideality in the mixing of cations in the octahedral sites of both muscovite and biotite. The quality of fit is indicated by a multiple correlation coefficient of 0.92. The standard deviation of 22 K in the residuals may be easily explained through the propagation of errors associated with microprobe analysis.

The geothermometric expression is given by Equation 10. Uncertainties associated with any application may be calculated at the desired confidence level using Equation 13. Applications of the muscovite-biotite geothermometer should be restricted to micas that are compositionally similar to those in the calibration data set.

REFERENCES CITED

Anderson, G.M. (1976) Error propagation by the Monte Carlo method in geochemical calculations. Geochimica et Cosmochimica Acta, 40, 1533–1538.
——— (1977) Uncertainties in calculations involving thermodynamic data. In H.J. Greenwood, Ed., Application of thermodynamics to petrology and ore deposits, p. 199–215. Mineralogical Association of Canada Short Course, vol. 2, Toronto, Canada.
Anderson, J.L., and Rowley, M.C. (1981) Synkinematic intrusion of peraluminous and associated metaluminous magmas, Whipple Mountains, California. Canadian Mineralogist, 19, 83–101.
Devore, J.L. (1982) Probability and statistics for engineering and the sciences, 640 p. Brooks/Cole, Monterey, California.
Ferry, J.M., and Spear, F.S. (1978) Experimental calibration of the partitioning of Fe and Mg between biotite and garnet. Contributions to Mineralogy and Petrology, 66, 113–117.
Fletcher, C.J.N., and Greenwood, H.J. (1979) Metamorphism and structure of the Penfold Creek area, near Quesnel Lake, British Columbia. Journal of Petrology, 20, 743–794.
Ganguly, J., and Kennedy, G.C. (1974) The energetics of natural garnet solid solution. Contributions to Mineralogy and Petrology, 48, 137–148.
Ganguly, J., and Saxena, S.K. (1984) Mixing properties of aluminosilicate garnets: Constraints from natural and experimental data, and applications to geothermo-barometry. American Mineralogist, 69, 88–97.
Grambling, J.A. (1986) A regional gradient in the composition of meta-

TABLE 4. Ranges of mica compositions in the calibration data set*

	K_{R1}^{ideal}	$X_{Mg}^{B} - X_{[6]Al}^{B}$	X_{Mg}^{B}	$X_{[6]Al}^{B}$	X_{Ti}^{B}	X_{Fe}^{B}	X_{Mg}^{M}
Minimum	0.108	0.165	0.319	0.089	0.0240	0.339	0.0085
Maximum	0.449	0.318	0.417	0.170	0.0732	0.443	0.0431

* Considers only the 39 samples used in the final regression.

morphic fluids in pelitic schist, Pecos Baldy, New Mexico. Contributions to Mineralogy and Petrology, 94, 149–164.

Guggenheim, E.A. (1967) Thermodynamics, 390 p. North-Holland, Amsterdam, Netherlands.

Guidotti, C.V. (1978) Compositional variation of muscovite in medium- to high-grade metapelites in northwestern Maine. American Mineralogist, 63, 878–884.

——— (1984) Micas in metamorphic rocks. Mineralogical Society of America Reviews in Mineralogy, 13, 357–456.

Guidotti, C.V., and Sassi, F.P. (1976) Muscovite as a petrogenetic indicator mineral in pelitic schist. Neues Jahrbuch für Mineralogie Abhandlungen, 27, 97–142.

Guidotti, C.V., Cheney, J.T., and Guggenheim, S. (1977) Distribution of titanium between coexisting muscovite and biotite in pelitic schists from northwestern Maine. American Mineralogist, 62, 438–448.

Hodges, K.V., and Crowley, P.D. (1985) Error estimation for empirical geothermometry for pelitic systems. American Mineralogist, 70, 702–709.

Hodges, K.V., and McKenna, L.W. (1987) Realistic propagation of uncertainties in geologic thermobarometry. American Mineralogist, 72, 671–680.

Hodges, K.V., and Spear, F.S. (1982) Geothermometry, geobarometry and the Al_2SiO_5 triple point at Mt. Moosilauke, New Hampshire. American Mineralogist, 67, 1118–1134.

Holdaway, M.J. (1971) Stability of andalusite and the aluminum silicate phase diagram. American Journal of Science, 271, 97–131.

Koziol, A.M., and Newton, R.C. (1988) Redetermination of the anorthite breakdown reaction and improvement of the plagioclase-garnet-Al_2SiO_5-quartz geobarometer. American Mineralogist, 73, 216–223.

Miller, C.F., Stoddard, E.F., Bradfish, L.J., and Dollase, W.A. (1981) Composition of plutonic muscovite: Genetic implications. Canadian Mineralogist, 19, 25–34.

Newton, R.C., and Haselton, H.T. (1981) Thermodynamics of the garnet-plagioclase-Al_2SiO_5-quartz geobarometer. In R.C. Newton, A. Navrotsky, and B.J. Wood, Eds., Thermodynamics of minerals and melts, p. 131–147. Springer-Verlag, New York.

Newton, R.C., Charlu, T.V., and Kleppa, O.J. (1980) Thermochemistry of the high structural state plagioclases. Geochimica et Cosmochimica Acta, 44, 933–941.

Pattison, D.R.M. (1987) Variations in Mg/(Mg + Fe), F, and (Fe,Mg)Si = 2Al in pelitic minerals in the Ballachulish thermal aureole, Scotland. American Mineralogist, 72, 255–272.

Pigage, L.C. (1976) Metamorphism of the Settler Schist, southwest of Yale, British Columbia. Canadian Journal of Earth Science, 13, 405–421.

——— (1982) Linear regression analysis of sillimanite-forming reactions at Azure Lake, British Columbia. Canadian Mineralogist, 20, 405–421.

Powell, R. (1978) Equilibrium thermodynamics in petrology, 284 p. Harper and Row, New York.

Price, J.G. (1985) Ideal site mixing in solid solutions, with an application to two-feldspar geothermometry. American Mineralogist, 70, 696–701.

Speer, J.A. (1984) Micas in igneous rocks. Mineralogical Society of America Reviews in Mineralogy, 13, 299–356.

Thompson, A.B. (1976) Mineral reactions in pelitic schist: I. Prediction of P-T-X (Fe-Mg) phase relations. American Journal of Science, 276, 401–424.

Tracy, R.J. (1978) High grade metamorphic reactions and partial melting in pelitic schist, west central Massachusetts. American Journal of Science, 278, 150–178.

Triboulet, C., and Audren, C. (1985) Continuous reactions between biotite, garnet, staurolite, kyanite-sillimanite-andalusite and P-T-time-deformation path in mica-schists from the estuary of the river Vilaine, South Brittany, France. Journal of Metamorphic Geology, 3, 91–105.